Robust Purely Optical Signatures of Floquet States in Laser-Dressed Crystals

Vishal Tiwari, Roman Korol, and Ignacio Franco, 1,2,3,*

Department of Chemistry, University of Rochester, Rochester, New York 14627, USA

Department of Physics and Astronomy, University of Rochester, Rochester, New York 14627, USA

Institute of Optics, University of Rochester, Rochester, New York 14627, USA

(Received 15 January 2025; revised 12 April 2025; accepted 6 October 2025; published 28 October 2025)

Strong light-matter interactions can create nonequilibrium materials with on-demand novel functionalities. For periodically driven solids, the Floquet-Bloch theory provides the natural states to characterize the physical properties of these laser-dressed systems. However, signatures of such Floquet states are needed, as common experimental conditions, such as pulsed laser excitation and dissipative many-body dynamics, can disrupt their formation and survival. Here, we identify a tell-tale signature of Floquet states in the linear optical response of laser-dressed solids that remains prominent even in the presence of the strong spectral congestion of bulk matter. To do so, we introduce a computationally efficient strategy based on the Floquet formalism to finally capture the full frequency dependence in the optical response properties of realistic laser-dressed crystals, and use it investigate the Floquet engineering in a first-principle model for ZnO of full dimensionality. The computations reveal intense, spectrally isolated, laser-controllable, absorption and stimulated emission features at midinfrared energies present for a wide range of laser-driving conditions that arise due to the hybridization of the Floquet states. As such, these spectral features open a purely optical pathway to investigate the birth and survival of Floquet states in crystals while avoiding the experimental challenges of fully reconstructing the band structure of laser-dressed materials.

DOI: 10.1103/5ywx-7dbs

Strong coupling of matter with light provides unprecedented opportunities for manipulating the physical properties of materials [1–7]. In particular, time-periodic lasers create laser-dressed solids, with emerging *nonequilibrium* properties that are most naturally understood through *stationary* populations of Floquet-Bloch states [8–13], that satisfy both the Floquet and Bloch theorem.

Because experimental realizations of Floquet engineering rarely satisfy the Floquet theorem—that requires unitary dynamics under strict periodic driving—there has been significant recent interest in identifying tell-tale signatures of the Floquet-Bloch states that can signal their birth and evolution under effects such as pulsed lasers and dissipative many-body dynamics that can disrupt their formation and survival. For this, time- and angle-resolved photoemission spectroscopy (Tr-ARPES) has emerged as a useful technique [14] to reconstruct the band structure and visualize the characteristic Floquet replicas [9,12,15–19], distorted copies of the electronic states separated in energy by multiples of the driving laser photon energy.

As an alternative, purely optical absorption experiments would be preferred as they are more common and often easier to realize experimentally. In the linear optical response of laser-dressed matter, the Floquet replicas lead to absorption sidebands that have been computationally

illustrated in model one-dimensional solids [13] and experimentally demonstrated in systems of low dimensionality [20–25]. However, in bulk materials, although the Floquet replicas have been observed in Tr-ARPES [16,17], they have remained elusive in the optical response, presumably because they are obscured by spectral congestion. This has prevented the use of optical absorption spectroscopy to study the emergence and evolution of Floquet states in materials.

Systematic progress requires developing a nonequilibrium theory of the linear response properties of laser-dressed solids and quantifying such a response in atomistically detailed models. According to the fluctuation-dissipation theorem, for near-equilibrium matter the response at frequency ω is dictated by the Fourier transform of one-time $\tau=t_2-t_1$ correlation functions $C(\tau)$ of the thermal state [26–28]. By contrast, for nonequilibrium laser-dressed materials, the response at frequency ω is now determined by a double Fourier transform of two-time correlation functions $C(t_1,t_2)$ because the time-translational symmetry is broken. This quantity is challenging to evaluate as it requires propagating the many-body quantum dynamics for long times forward and back for each pair of times t_1 and t_2 [13,29].

In this Letter, we demonstrate the first computations of the nonequilibrium optical absorption spectra of a realistic laser-dressed three-dimensional solid, ZnO, described using a first-principle density functional theory (DFT)

^{*}Contact author: ignacio.franco@rochester.edu

Hamiltonian. As detailed in our companion paper [30], these computations are now feasible due to the development of (i) a Floquet-based approach to efficiently compute the full frequency dependence of the optical response of laser-dressed solids; (ii) a truncated velocity gauge for the light-matter interactions that enables the use of firstprinciple Hamiltonians and overcomes well-known convergence issues of the velocity gauge with the number of bands [31–33]; (iii) the massively parallel computational implementation of the theory; and (iv) its integration with electronic structure codes for solids [34]. Our computations reveal robust, laser-controllable, spectrally isolated, intense optical features at midinfrared frequencies that provide a purely optical tell-tale signature of the emergence of Floquet states. These features can be used to monitor their birth and evolution in solids through optical absorption spectroscopy.

We simulate a drive-probe physical situation in which a continuous-wave laser of arbitrary intensity and frequency drives a solid of arbitrary band structure and dimensionality out of equilibrium. The effective absorption properties of this laser-dressed solid are then probed by a weak continuous-wave laser source. We treat the drive laser exactly through a Floquet formalism while the influence of the probe is captured to first order in perturbation theory. In our companion paper [30], we detail the underlying theory and computational framework to compute the frequency-dependent optical absorption spectra of laser-dressed solids using first-principle Hamiltonians.

Briefly, the total Hamiltonian is $\hat{H}(t) = \hat{H}_{LD}(t) +$ $\hat{H}_{\rm p}(t)$, where $\hat{H}_{\rm LD}(t)$ describes the material and its interaction with a drive laser $\mathbf{E}_{\rm d}(t) = \hat{\mathbf{e}}_{\rm d} E_{\rm d} \cos(\Omega t)$ with period $T = 2\pi/\Omega$, frequency Ω , amplitude $E_{\rm d}$, and polarization $\hat{\bf e}_{\rm d}$. In turn, $\hat{H}_{p}(t)$ describes the interaction with the probe laser $\mathbf{E}_{\mathrm{p}}(t) = \hat{\mathbf{e}}_{\mathrm{p}} E_{\mathrm{p}} \cos(\omega t)$ of amplitude E_{p} , frequency ω , and polarization $\hat{\mathbf{e}}_{\mathrm{p}}$. We consider the effect of the drive laser exactly while the influence of the probe is captured to first order in perturbation theory. In second quantization, $\hat{H}_{\mathrm{LD}}(t) = \sum_{\mathbf{k} \in \mathrm{BZ}} \sum_{u,v} \langle \psi_{u\mathbf{k}} | \hat{\mathcal{H}}_{\mathrm{LD}}(t) | \psi_{v\mathbf{k}} \rangle \hat{c}_{u\mathbf{k}}^{\dagger} \hat{c}_{v\mathbf{k}}, \quad \text{where}$ $\hat{\mathcal{H}}_{\mathrm{LD}}(t)$ is the single-particle laser-dressed Hamiltonian. Here, $\hat{c}_{u\mathbf{k}}^{\dagger}(\hat{c}_{u\mathbf{k}})$ creates (annihilates) a fermion in Bloch state $|\psi_{u\mathbf{k}}\rangle = V^{-1/2}e^{i\mathbf{k}\cdot\hat{\mathbf{r}}}|u\mathbf{k}\rangle$ with band index u, and crystal momentum **k** in the first Brillouin zone (BZ), where $|u\mathbf{k}\rangle$ is the Bloch mode and V the crystal's volume. Since $\hat{\mathcal{H}}_{\mathrm{LD}}(t) = \hat{\mathcal{H}}_{\mathrm{LD}}(t+T)$ is time periodic, we can invoke the Floquet theorem where now the Floquet-Bloch states $|\Psi_{\alpha \mathbf{k}}(t)\rangle = V^{-1/2} e^{-iE_{\alpha \mathbf{k}}t/\hbar} e^{i\mathbf{k}\cdot\hat{\mathbf{r}}} |\Phi_{\alpha \mathbf{k}}(t)\rangle$ are solutions to the time-dependent Schrödinger equation $[i\hbar(\partial/\partial t)|\Psi_{\alpha \mathbf{k}}(t)\rangle =$ $\hat{\mathcal{H}}_{LD}(t)|\Psi_{\alpha \mathbf{k}}(t)\rangle$. The quasienergies $\{E_{\alpha \mathbf{k}}\}$ and Floquet-Bloch modes $\{|\Phi_{\alpha \mathbf{k}}(t)\rangle\}$ are solutions to the eigenvalue problem $[i\hbar(\partial/\partial t) - \hat{\mathcal{H}}_{LD}(t)]|\Phi_{\alpha \mathbf{k}}(t)\rangle = E_{\alpha \mathbf{k}}|\Phi_{\alpha \mathbf{k}}(t)\rangle$ in Sambe space [35]. The quasienergies are uniquely defined in the first Floquet-Brillouin zone (FBZ) such that $-\hbar\Omega/2 \le E_{\alpha \mathbf{k}} < \hbar\Omega/2$ for $\mathbf{k} \in BZ$. The Floquet-Bloch modes are time periodic with period T and space periodic with period \mathbf{R} —the lattice vector of the crystal.

The nonequilibrium optical absorption coefficient of a laser-dressed crystal at probe photon energy $\hbar\omega$ is [30]

$$\begin{split} A(\omega) &= \frac{e^2 \pi}{m_e^2 \epsilon_0 c n_r V \omega} \sum_{\mathbf{k} \in \mathrm{BZ}} \sum_{\alpha, \beta} \sum_n \Lambda_{\alpha \beta \mathbf{k}} |\mathcal{Z}_{\alpha \beta \mathbf{k}}^{(n)}|^2 \\ &\times \left[\delta (E_{\alpha \beta \mathbf{k}} + n \hbar \Omega - \hbar \omega) - \delta (E_{\alpha \beta \mathbf{k}} + n \hbar \Omega + \hbar \omega) \right]. \end{split} \tag{1}$$

Here, ϵ_0 is the vacuum's electric permittivity, c the speed of light, and n_r the material's refractive index. The quantity $E_{\alpha\beta\mathbf{k}}=E_{\alpha\mathbf{k}}-E_{\beta\mathbf{k}}$ is the Bohr transition energy between Floquet-Bloch mode α and β at crystal momentum \mathbf{k} . The population factor $\Lambda_{\alpha\beta\mathbf{k}}=V^{-4}\sum_{u',u}|\langle u\mathbf{k}|\Phi_{\beta\mathbf{k}}(t_0)\rangle|^2|\langle\Phi_{\alpha\mathbf{k}}(t_0)|u'\mathbf{k}\rangle|^2\bar{n}_{u\mathbf{k}}(1-\bar{n}_{u'\mathbf{k}}),$ where $\bar{n}_{u\mathbf{k}}=\langle\psi(t_0)|\hat{c}_{u\mathbf{k}}^{\dagger}\hat{c}_{u\mathbf{k}}|\psi(t_0)\rangle$ is the occupation number of band u and crystal momentum \mathbf{k} of many-body state $|\psi(t_0)\rangle$ at preparation time t_0 . In turn, $\mathcal{Z}_{\alpha\beta\mathbf{k}}^{(n)}$ is the nth Fourier component of the truncated momentum matrix element $\mathcal{Z}_{\alpha\beta\mathbf{k}}(t)=V^{-1}\langle\Phi_{\alpha\mathbf{k}}(t)|e^{-i\mathbf{k}\cdot\hat{\mathbf{r}}}\hat{z}(t)e^{i\mathbf{k}\cdot\hat{\mathbf{r}}}|\Phi_{\beta\mathbf{k}}(t)\rangle$ between the Floquet-Bloch mode α and β at crystal momentum \mathbf{k} , where $\hat{z}(t)$ is the truncated momentum operator [cf. Eq. (14) in Ref. [30]].

Equation (1) is valid for any arbitrary time-periodic driving laser and for any space-periodic material including semiconductors, semimetals, insulators, and quantum materials. When interfaced with DFT computations, it captures electronic correlations at preparation time. Remarkably, its structure is analogous to the near-equilibrium optical response [36] but with the Floquet-Bloch modes playing the role of the pristine eigenstates. Specifically, optical absorption in laser-dressed solids arises due to transitions among Floquet-Bloch modes $\beta \rightarrow \alpha$ separated by n Floquet-Brillouin zones with Bohr transition energy $E_{\alpha\beta\mathbf{k}} + n\hbar\Omega$. Here $n = 0, \pm 1, ..., \pm n_F$ where $2n_F + 1$ is the maximum number of FBZs needed for convergence. The first term represents absorption, the second stimulated emission. Transition intensities are determined by the population factor $\Lambda_{\alpha\beta\mathbf{k}}$ (that guarantees transitions occur from an occupied to an empty state) and the momentum matrix element $\mathcal{Z}^{(n)}_{\alpha\beta\mathbf{k}}$ (that are dependent on the number n of FBZs separating the modes). Interestingly, in this nonequilibrium context, transition matrix elements and population factors depend on the strength and nature of the driving laser (instead of being properties inherent to the material only), and optical transitions occur among states that can be separated by a variable number of FBZs leading to absorption sidebands.

To find optical signatures of Floquet states, we use Eq. (1) to compute the absorption spectrum for the laser-dressed wurtzite ZnO crystal using a first-principle

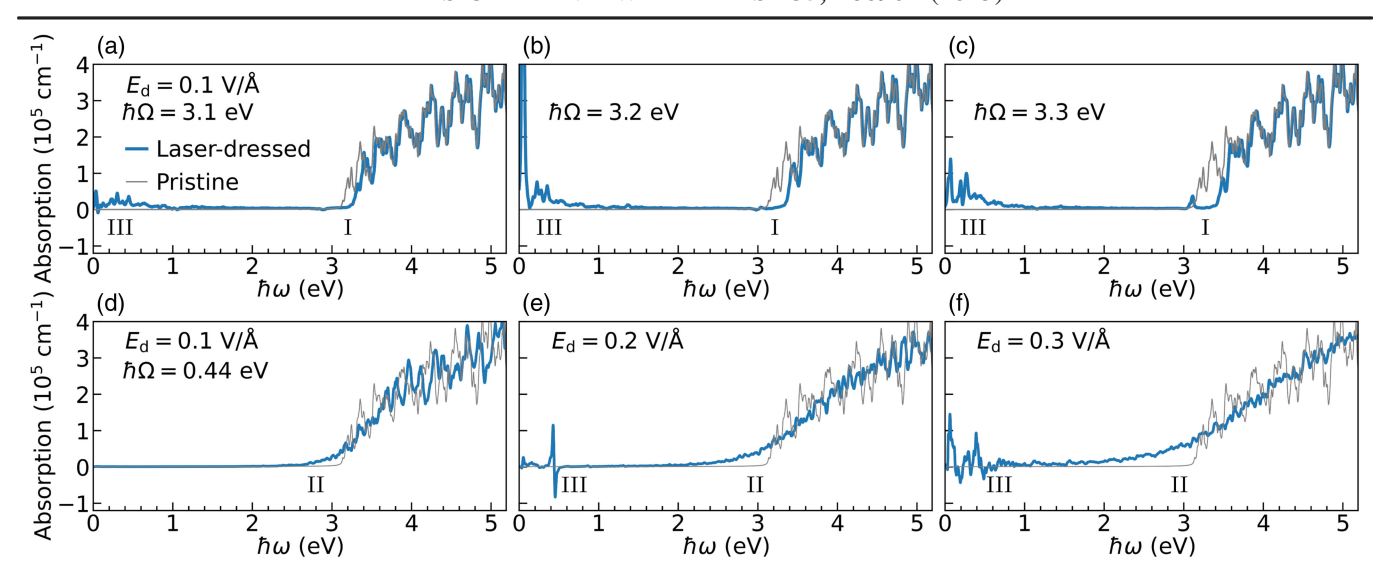


FIG. 1. Frequency (ω) dependence of the optical absorption spectrum $A(\omega)n_r$ for ZnO dressed with near resonant (a)–(c) and off resonance (d)–(f) light of photon energy $\hbar\Omega$ and amplitude $E_{\rm d}$ (blue lines). Gray lines: spectra of pristine solid. Floquet engineering leads to strong modification of the optical response, including band-gap renormalization (feature I), below band-gap absorption (II), and the emergence of midinfrared features (III).

Hamiltonian and the computational strategy detailed in Ref. [30]. The large ~3.2 eV ZnO band gap enables resonant and nonresonant laser dressing using experimentally accessible frequencies [37,38]. The DFT electronic structure of ZnO was computed using Quantum Espresso [39] with Hubbard (DFT + U) corrections needed to reproduce experimental band gaps [40–42] followed by a Wannier interpolation using Wannier90 [43] that enables efficient computation of Eq. (1). The employed 22-Wannier model accurately reproduces the DFT band structure in a 25 eV energy range (see Fig. S1 in the Supplemental Material [44]) and, together with $n_{\rm F} = 301$ and a dense **k**-space grid grid of (30)³, provides converged results for the nonequilibrium optical absorption. Throughout, since electronphonon interactions introduce Franck-Condon like progressions [45], in our computations spectral features are Lorentzian broadened with width 0.02 eV. Further, transitions with energy less than 0.06 eV are not reported to account for the limits of the finite BZ discretization. We take the drive and probe to be linearly polarized along the crystal's c-axis. Other polarization directions yield qualitatively similar physics. Additional computational details are included in the Supplemental Material [44].

Figure 1 shows the optical absorption spectra of pristine ZnO (gray lines) and laser-dressed (blue lines) ZnO with field amplitudes $E_{\rm d}=0.1$ –0.3 V/Å (intensities 0.13-1.2 TW/cm²) in the intermediate regime of light-matter interaction (nonionizing, but nonperturbative) and with frequency chosen to be near-resonance with the bandedge [$\hbar\Omega=3.1$ –3.3 eV, Figs. 1(a)–1(c)] and off-resonance [$\hbar\Omega=0.44$ eV, Figs. 1(d)–1(f)]. The pristine spectrum shows a sharp band-edge at 3.2 eV as observed experimentally [38,42]. As seen, Floquet engineering leads to strong modification of the optical response.

In the near-resonance case [Figs. 1(a)-1(c)], the laserdressing strongly suppresses the absorption for $\hbar\omega \approx \hbar\Omega$ (feature I) and leaves the spectrum for $\hbar\omega > 4 \text{ eV}$ unchanged. This suppression is due to the band-gap renormalization created by hybridization of the Floquet-Bloch states (see associated Tr-ARPES evidence in Ref. [17]). More explicitly, when the solid is resonantly driven, the first Floquet replica of the valence (conduction) band overlaps with the conduction (valence) band. This leads to band hybridization that opens an energy gap at $\hbar\omega \approx \hbar\Omega$, thus removing transitions at this frequency. This band-gap renormalization is an optical signal of the formation of Floquet states as it occurs due to their hybridization. However, the challenge with isolating this feature in the optical spectra is that it emerges for $\hbar\omega$ around the band-edge where it can be obscured by excitonic features [46–48] which are not included in the model.

For off-resonance driving [Figs. 1(d)–1(f)], the laserdressing leads to below band-edge absorption features $\hbar\omega$ < 3.2 eV (II) that spread to even lower energies as the field strength is increased. This so-called dynamical Franz-Keldysh Effect [49] can be attributed to transitions occurring among the Floquet replicas of valence and conduction bands [13]. For off-resonance drive laser, multiple Floquet replicas are formed leading to transitions with energies lower than the field-free band-edge. Further, since the replicas are separated from each other by the drive photon energy, they can lead to absorption sidebands. Both the below-band gap features and the sidebands are optical signatures of Floquet states. However, as the band renormalization, they are also challenging to observe. Below-band gap absorption overlaps in energy with dominant exciton features. In turn, while the absorption sidebands are expected from Eq. (1), and clearly visible in systems of low-dimensionality [23] including one-dimensional model crystals [13], they are obscured in Figs. 1(d)–1(f) by the spectral congestion of this three-dimensional material.

Are there any features in the laser-dressed optical spectrum that remain visible in realistic systems?

Interestingly, Fig. 1 shows prominent absorption and stimulated emission features (III) at mid-infrared frequencies ($\hbar\omega$ < 0.6 eV) that emerge under both near-resonance [Figs. 1(a)–1(c)] and off-resonance [Figs. (1e) and 1(f)] driving. These features are well separated from the bandedge or vibrational features, and are thus not obscured by possible excitonic contribution or spectral congestion. Further, their emergence is robust to changes in the drive laser frequency and amplitude.

To clarify their physical origin, we developed a minimal one-dimensional two-band model that captures this phenomenon from a projection of the highest valence and the lowest conduction band of ZnO constructed using $\mathbf{k} \cdot \mathbf{p}$ perturbation theory [50] (see the Supplemental Material [44] for model parameters). This model system also shows low-frequency transitions for the same drive laser parameters as ZnO (see Fig. S3 in the Supplemental Material [44]). However, its reduced dimensionality enables one to more clearly identify the essential physics.

As we now show, these low-frequency features arise due to formation and subsequent hybridization of the Floquet-Bloch modes. The top row of Fig. 2 shows this for drive laser frequency near resonant to the band edge. We plot the quasienergies of the two-band model within a FBZ for a representative k point (k = 0.1 units of $2\pi/a$, with a =5.2 Å the unit cell length) in Fig. 2(a) as a function of $\hbar\Omega$. The two quasienergies form an avoided crossing around $\hbar\Omega = 3.4$ eV which is a signature of level hybridization. The absorption spectrum of this two-band model with driving frequency chosen before the avoided crossing $[\hbar\Omega = 2.9 \text{ eV purple vertical line in Fig. 2(a)}]$, shown in Fig. 2(c) (purple line) shows no significant low-frequency feature. But when the model is driven by laser parameters chosen at the avoided crossing [$\hbar\Omega = 3.4$ eV green vertical line in Fig. 2(a)], the spectrum [Fig. 2(c) green line] exhibits an intense low-frequency absorption feature centered at $\hbar\omega = 0.2$ eV with strong contribution from the transition at k = 0.1.

Similar behavior is also seen for the off resonance drive laser with $\hbar\Omega=0.44$ eV. The two quasienergies in a FBZ for the same representative k=0.1 as a function of $E_{\rm d}$ in Fig. 2(b) show an avoided crossing centered around $E_{\rm d}=0.253$ V/Å. When the model is driven by laser with $E_{\rm d}=0.238$ V/Å before the avoided crossing [purple vertical line in Fig. 2(b)], the spectrum shown in Fig. 2(d) (purple line) shows no significant low-frequency features in general and a faint transition for k=0.1 in particular. But when the system is driven by a laser with $E_{\rm d}=0.25$ V/Å at the avoided crossing [green vertical line in Fig. 2(b)], the

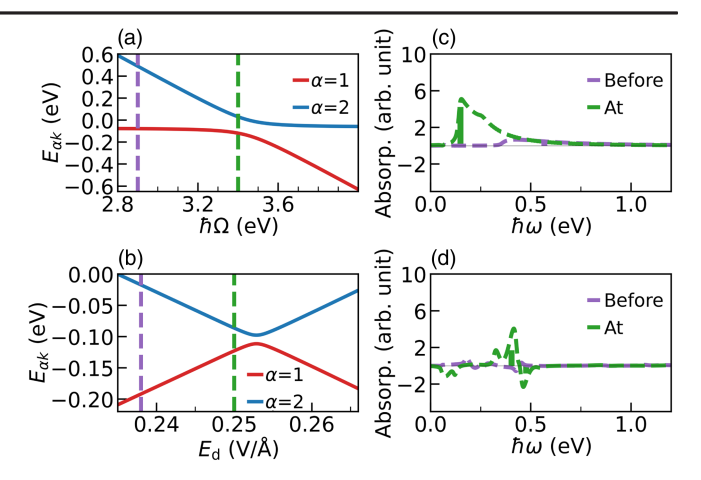


FIG. 2. Low-frequency transitions in the optical response as demonstrated in a minimal two-band model for near resonance (top row) and off resonance (bottom row) driving. (a)–(b) Quasienergies at a representative k=0.1 showing the avoided crossing as a function of (a) driving laser frequency $\hbar\Omega$ (with fixed $E_{\rm d}=0.1$ V/Å) and (b) amplitude $E_{\rm d}$ (with fixed $\hbar\Omega=0.44$ eV). Vertical purple and green lines mark parameters before or at the avoided crossing, respectively. Panels (c) [or (d)] show the absorption spectra corresponding to (a) [or (b)] before (purple) and at (green) the avoided crossing. Transition lines signal the k=0.1 contribution only. Note that the low-frequency transitions emerge in the avoided crossing region where Floquet states hybridize.

spectrum shown in Fig. 2(d) (green line) shows intense absorption and stimulated emission features. This shows that in both a resonantly and nonresonantly driven solid, the hybridization of the Floquet-Bloch modes indicated by the opening of avoided crossings induces low-frequency transition signals.

Figures 3(a) and 3(b) summarize the emergent physical picture. Laser dressing leads to the formation of Floquet replicas (blue lines) of the valence and conduction band (black lines) that can energetically overlap either with the original Bloch bands or their replicas. This induces hybridization of the Floquet-Bloch states and formation of hybrid bands (red lines) that display avoided crossings as a function of laser parameters [Figs. 2(a) and 2(b)]. Probing this laser-dressed band structure leads to intense lowfrequency transitions as indicated by the purple arrows. For the resonant case, Fig. 3(a), the low-frequency features arise because of intra FBZ (n = 0 in Eq. (1) optical)transitions. In turn, for the nonresonant case Fig. 3(b), such features can arise because of intra (n = 0) and inter FBZ $(n = \pm 1)$ optical transitions for the inter FBZ transition n = 1 leads to absorption and n = -1 leads to stimulated emission resulting in the characteristic double peak in Fig. 2(d) around $\hbar\omega \approx \hbar\Omega$ [see also the same feature in Fig. 1(e)], with the lower frequency peak yielding absorption and the higher-frequency one stimulated emission. Higher order transitions are possible but less prominent in the spectra for this laser dressing. All these features

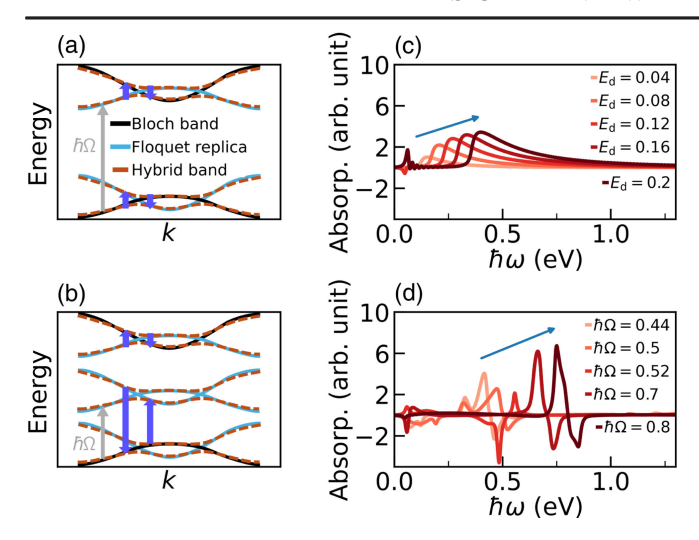


FIG. 3. (a)–(b) Schematic of the laser-dressed band structure showing the emergence of the low-frequency transitions due to Floquet hybridization for (a) resonant and (b) nonresonant driving. Purple arrows signal possible low-frequency transitions. These transitions blueshift with increasing driving laser's (c) amplitude $E_{\rm d}$ in V/Å for resonant driving ($\hbar\Omega=3.1~{\rm eV}$) and (d) frequency $\hbar\Omega$ in eV ($E_{\rm d}=0.25~{\rm V/Å}$) for nonresonant driving.

emerge because of the hybridization of Floquet-Bloch modes; see Fig. 2.

Figures 3(a) and 3(b) suggest that these low-frequency features are controllable simply by varying the parameters of the driving laser. This is, in fact, clearly shown in computations in the two-band model shown in Figs. 3(c) and 3(d). For resonant driving [Fig. 3(c)], increasing the laser amplitude blueshifts the low-frequency features in the spectra (blue arrow). This is because the gap due to Floquet hybridization increases with the strength of the light-matter interactions, akin to the Autler-Townes effect [51,52]. In turn, for nonresonant driving [Fig. 3(d)], the low-frequency feature due to inter FBZ transition ($n = \pm 1$) blueshift upon increasing the drive laser frequency. This controllability can be used to characterize the emergent low-frequency features, and enable their resolution with ultrafast probes.

This origin of the low-frequency features in the two-band model can be naturally extended to the realistic laser-dressed ZnO. Figure 2 shows that for a single k point, the two Floquet-Bloch modes form an avoided crossing in the band structure due to hybridization for certain drive laser parameters. In the realistic computations, similar hybridization occurs but for a large number of \mathbf{k} vectors given that a sufficient driving laser amplitude is applied. This leads to a plethora of low-frequency transitions, some that lead to absorption while others lead to stimulated emission depending on whether the laser parameters are before or after each specific avoided crossing. These contributions do not exactly cancel one another leading to the robust low-frequency features observed in Fig. 1.

In nature, these low-frequency features will arise from the hybridization of many-body Floquet replicas. For this reason, as illustrated for a Hubbard-Holstein model [53–56] in Figs. S4-S7 in the Supplemental Material [44] using exact diagonalization techniques [57–60], electron correlations and electron-phonon couplings influence the frequency and magnitude of these transitions as they modulate the many-body Floquet states but do not obscure the effect. Further, the effect is robust to spectral broadening. In fact, as shown in Fig. S8 in the Supplemental Material [44], increasing spectral broadening in a wide range of energies (0.02–0.2 eV) reduces but does not obscure the main low-frequency features.

These low-frequency features are a clear indication of the formation of Floquet states in laser-dressed materials. Our computations suggest that to observe them in semiconductors requires moderate field intensities (~0.13 TW/cm²) for lasers with frequency near resonant to the band edge or stronger lasers (~1.2 TW/cm²) if dressing off resonance.

Dissipation, pulsed excitation, and other effects that limit the applicability of the Floquet theory are expected to reduce the visibility of these low-frequency features. Thus, the onset and disappearance of these laser-controllable low-frequency features can be used to test the applicability of Floquet engineering in crystals under experimentally relevant conditions. In particular, we expect that the optical controllability of these low-frequency features can be employed to characterize time scales of effects that break the Hamiltonian's time periodicity.

To summarize, we presented the first computational demonstration of the nonequilibrium optical absorption spectrum of a laser-dressed solid (ZnO) described using a first-principle electronic structure of full dimensionality. We show that the Floquet engineering can dramatically change the optical response of a crystal. In particular, we find prominent absorption and stimulated emission features at midinfrared frequencies that are robust to drive laser parameters, survive the spectral congestion and broadening in solids, and are well isolated from the field-free band edge and possible excitonic transitions. Using a minimalistic two-band model, we demonstrated that these features arise due to the hybridization of the Floquet states. We propose that these features provide a robust, laser-controllable, purely optical tell-tale signature of the formation of Floquet states in nonequilibrium bulk matter that can be used to study the validity of Floquet engineering with varying experimental conditions (i.e., temperature, material, pulse width, etc.). As such, these spectral features open a purely optical pathway to investigate the birth and survival of Floquet states while avoiding the experimental challenges of fully reconstructing the band structure of laser-dressed materials.

Acknowledgments—This research is based upon work supported by the National Science Foundation under Grant

No. CHE-2416048. V. T. acknowledges the DeRight fellowship support from the University of Rochester.

Data availability—The data that support the findings of this article are openly available [61].

- [1] T. Oka and S. Kitamura, Floquet engineering of quantum materials, Annu. Rev. Condens. Matter Phys. **10**, 387 (2019).
- [2] J. B. Curtis, Z. M. Raines, A. A. Allocca, M. Hafezi, and V. M. Galitski, Cavity quantum Eliashberg enhancement of superconductivity, Phys. Rev. Lett. 122, 167002 (2019).
- [3] A. de la Torre, D. M. Kennes, M. Claassen, S. Gerber, J. W. McIver, and M. A. Sentef, Colloquium: Nonthermal pathways to ultrafast control in quantum materials, Rev. Mod. Phys. 93, 041002 (2021).
- [4] M. Budden, T. Gebert, M. Buzzi, G. Jotzu, E. Wang, T. Matsuyama, G. Meier, Y. Laplace, D. Pontiroli, M. Riccò, F. Schlawin, D. Jaksch, and A. Cavalleri, Evidence for metastable photo-induced superconductivity in K₃C₆₀, Nat. Phys. 17, 611 (2021).
- [5] C. Bao, P. Tang, D. Sun, and S. Zhou, Light-induced emergent phenomena in 2D materials and topological materials, Nat. Rev. Phys. 4, 33 (2021).
- [6] F. J. Garcia-Vidal, C. Ciuti, and T. W. Ebbesen, Manipulating matter by strong coupling to vacuum fields, Science 373, eabd0336 (2021).
- [7] I. Tyulnev, Álvaro. Jiménez-Galán, J. Poborska, L. Vamos, P. S. J. Russell, F. Tani, O. Smirnova, M. Ivanov, R. E. F. Silva, and J. Biegert, Valleytronics in bulk MoS₂ with a topologic optical field, Nature (London) 628, 746 (2024).
- [8] F. H. M. Faisal and J. Z. Kamiński, Floquet-Bloch theory of high-harmonic generation in periodic structures, Phys. Rev. A 56, 748 (1997).
- [9] Y. H. Wang, H. Steinberg, P. Jarillo-Herrero, and N. Gedik, Observation of Floquet-Bloch states on the surface of a topological insulator, Science 342, 453 (2013).
- [10] J.-Y. Shan, M. Ye, H. Chu, S. Lee, J.-G. Park, L. Balents, and D. Hsieh, Giant modulation of optical nonlinearity by Floquet engineering, Nature (London) 600, 235 (2021).
- [11] S. K. Earl, M. A. Conway, J. B. Muir, M. Wurdack, E. A. Ostrovskaya, J. O. Tollerud, and J. A. Davis, Coherent dynamics of Floquet-Bloch states in monolayer WS₂ reveals fast adiabatic switching, Phys. Rev. B 104, L060303 (2021).
- [12] S. Aeschlimann, S. A. Sato, R. Krause, M. Chávez-Cervantes, U. De Giovannini, H. Hübener, S. Forti, C. Coletti, K. Hanff, K. Rossnagel, A. Rubio, and I. Gierz, Survival of Floquet–Bloch states in the presence of scattering, Nano Lett. 21, 5028 (2021).
- [13] V. Tiwari, B. Gu, and I. Franco, Floquet theory and computational method for the optical absorption of laserdressed solids, Phys. Rev. B 108, 064308 (2023).
- [14] F. Boschini, M. Zonno, and A. Damascelli, Time-resolved ARPES studies of quantum materials, Rev. Mod. Phys. 96, 015003 (2024).
- [15] S. Ito, M. Schüler, M. Meierhofer, S. Schlauderer, J. Freudenstein, J. Reimann, D. Afanasiev, K. A. Kokh, O. E. Tereshchenko, J. Güdde, M. A. Sentef, U. Höfer, and R. Huber, Build-up and dephasing of Floquet–Bloch

- bands on subcycle timescales, Nature (London) **616**, 696 (2023).
- [16] S. Zhou, C. Bao, B. Fan, F. Wang, H. Zhong, H. Zhang, P. Tang, W. Duan, and S. Zhou, Floquet engineering of black phosphorus upon below-gap pumping, Phys. Rev. Lett. 131, 116401 (2023).
- [17] S. Zhou, C. Bao, B. Fan, H. Zhou, Q. Gao, H. Zhong, T. Lin, H. Liu, P. Yu, P. Tang, S. Meng, W. Duan, and S. Zhou, Pseudospin-selective Floquet band engineering in black phosphorus, Nature (London) 614, 75 (2023).
- [18] D. Choi, M. Mogi, U. De Giovannini, D. Azoury, B. Lv, Y. Su, H. Hübener, A. Rubio, and N. Gedik, Observation of Floquet—Bloch states in monolayer graphene, Nat. Phys. 21, 1100 (2025).
- [19] M. Merboldt, M. Schüler, D. Schmitt, J. P. Bange, W. Bennecke, K. Gadge, K. Pierz, H. W. Schumacher, D. Momeni, D. Steil, S. R. Manmana, M. Sentef, M. Reutzel, and S. Mathias, Observation of Floquet states in graphene, Nat. Phys. 21, 1093 (2025).
- [20] C. Deng, J.-L. Orgiazzi, F. Shen, S. Ashhab, and A. Lupascu, Observation of floquet states in a strongly driven artificial atom, Phys. Rev. Lett. **115**, 133601 (2015).
- [21] J. V. Koski, A. J. Landig, A. Pályi, P. Scarlino, C. Reichl, W. Wegscheider, G. Burkard, A. Wallraff, K. Ensslin, and T. Ihn, Floquet spectroscopy of a strongly driven quantum dot charge qubit with a microwave resonator, Phys. Rev. Lett. 121, 043603 (2018).
- [22] S. Park, W. Lee, S. Jang, Y.-B. Choi, J. Park, W. Jung, K. Watanabe, T. Taniguchi, G. Y. Cho, and G.-H. Lee, Steady Floquet–Andreev states in graphene Josephson junctions, Nature (London) **603**, 421 (2022).
- [23] Y. Kobayashi, C. Heide, A. C. Johnson, V. Tiwari, F. Liu, D. A. Reis, T. F. Heinz, and S. Ghimire, Floquet engineering of strongly driven excitons in monolayer tungsten disulfide, Nat. Phys. 19, 171 (2023).
- [24] K. Boos, S. K. Kim, T. Bracht, F. Sbresny, J. M. Kaspari, M. Cygorek, H. Riedl, F. W. Bopp, W. Rauhaus, C. Calcagno, J. J. Finley, D. E. Reiter, and K. Müller, Signatures of dynamically dressed states, Phys. Rev. Lett. 132, 053602 (2024).
- [25] Y. Li, Y. Yang, Y. Liu, J. Zhu, and K. Wu, Observation of Floquet states and their dephasing in colloidal nanoplatelets driven by visible pulses, Nat. Photonics 18, 1044 (2024).
- [26] R. Kubo, Stochastic Liouville equations, J. Math. Phys. (N.Y.) 4, 174 (1963).
- [27] R. Kubo, Statistical-mechanical theory of irreversible processes. I. General theory and simple applications to magnetic and conduction problems, J. Phys. Soc. Jpn. 12, 570 (1957).
- [28] S. Mukamel, Principles of Nonlinear Optical Spectroscopy, Oxford series in optical and imaging sciences (Oxford University Press, New York, 1995).
- [29] B. Gu and I. Franco, Optical absorption properties of laserdriven matter, Phys. Rev. A 98, 063412 (2018).
- [30] V. Tiwari and I. Franco, First-principle-based Floquet engineering of solids in the velocity gauge, Phys. Rev. B **112**, 085139 (2025).
- [31] K. S. Virk and J. E. Sipe, Semiconductor optics in length gauge: A general numerical approach, Phys. Rev. B **76**, 035213 (2007).

- [32] V. S. Yakovlev and M. S. Wismer, Adiabatic corrections for velocity-gauge simulations of electron dynamics in periodic potentials, Comput. Phys. Commun. 217, 82 (2017).
- [33] A. Taghizadeh, F. Hipolito, and T. G. Pedersen, Linear and nonlinear optical response of crystals using length and velocity gauges: Effect of basis truncation, Phys. Rev. B **96**, 195413 (2017).
- [34] FloqticS (Floquet optics in Solids)—Code for computing the optical absorption spectrum of laser-dressed solids, https://github.com/ifgroup/floqtics.
- [35] H. Sambe, Steady states and quasienergies of a quantummechanical system in an oscillating field, Phys. Rev. A 7, 2203 (1973).
- [36] M. Dresselhaus, G. Dresselhaus, S. Cronin, and A. G. S. Filho, *Solid State Properties* (Springer, Berlin, Heidelberg, 2018).
- [37] S. Ghimire, A. D. DiChiara, E. Sistrunk, P. Agostini, L. F. DiMauro, and D. A. Reis, Observation of high-order harmonic generation in a bulk crystal, Nat. Phys. 7, 138 (2010).
- [38] S. Ghimire, A. D. DiChiara, E. Sistrunk, U. B. Szafruga, P. Agostini, L. F. DiMauro, and D. A. Reis, Redshift in the optical absorption of ZNO single crystals in the presence of an intense midinfrared laser field, Phys. Rev. Lett. 107, 167407 (2011).
- [39] P. Giannozzi *et al.*, Advanced capabilities for materials modelling with Quantum Espresso, J. Phys. Condens. Matter 29, 465901 (2017).
- [40] A. Janotti, D. Segev, and C. G. Van de Walle, Effects of cation d states on the structural and electronic properties of III-nitride and II-oxide wide-band-gap semiconductors, Phys. Rev. B 74, 045202 (2006).
- [41] A. Calzolari, A. Ruini, and A. Catellani, Anchor group versus conjugation: Toward the gap-state engineering of functionalized ZNO(1010) surface for optoelectronic applications, J. Am. Chem. Soc. 133, 5893 (2011).
- [42] J. A. Spencer, A. L. Mock, A. G. Jacobs, M. Schubert, Y. Zhang, and M. J. Tadjer, A review of band structure and material properties of transparent conducting and semi-conducting oxides: Ga₂O₃, Al₂O₃, In₂O₃, ZnO, SnO2, CdO, NiO, CuO, and Sc₂O₃, Appl. Phys. Rev. 9, 011315 (2022).
- [43] G. Pizzi et al., wannier90 as a community code: New features and applications, J. Phys. Condens. Matter 32, 165902 (2020).
- [44] See Supplemental Material at http://link.aps.org/supplemental/10.1103/5ywx-7dbs for ZnO electronic structure computation, two-band model parameters, optical response of laser-dressed two-band model, optical response of laser-dressed Hubbard-Holstein model, and absorption spectra of laser-dressed ZnO with varying spectral broadening.

- [45] T. Szidarovszky, A. G. Csaszar, G. J. Halasz, and A. Vibok, Rovibronic spectra of molecules dressed by light fields, Phys. Rev. A 100, 033414 (2019).
- [46] D. C. Reynolds, D. C. Look, B. Jogai, C. W. Litton, G. Cantwell, and W. C. Harsch, Valence-band ordering in ZnO, Phys. Rev. B 60, 2340 (1999).
- [47] U. Ozgur, Y. I. Alivov, C. Liu, A. Teke, M. A. Reshchikov, S. Dogan, V. Avrutin, S.-J. Cho, and H. Morkoc, A comprehensive review of ZNO materials and devices, J. Appl. Phys. 98, 041301 (2005).
- [48] M. Rohlfing and S. G. Louie, Electron-hole excitations and optical spectra from first principles, Phys. Rev. B **62**, 4927 (2000).
- [49] A. P. Jauho and K. Johnsen, Dynamical Franz-Keldysh effect, Phys. Rev. Lett. 76, 4576 (1996).
- [50] H. Haug and S. W. Koch, Quantum Theory of the Optical and Electronic Properties of Semiconductors (World Scientific, Singapore, 2009), 10.1142/7184.
- [51] S. H. Autler and C. H. Townes, Stark effect in rapidly varying fields, Phys. Rev. 100, 703 (1955).
- [52] J. Kim, J. S. Lim, H.-R. Noh, and S. K. Kim, Experimental observation of the Autler–Townes splitting in polyatomic molecules, J. Phys. Chem. Lett. 11, 6791 (2020).
- [53] M. Schüler, M. Eckstein, and P. Werner, Truncating the memory time in nonequilibrium dynamical mean field theory calculations, Phys. Rev. B 97, 245129 (2018).
- [54] S. Johnston, F. Vernay, B. Moritz, Z.-X. Shen, N. Nagaosa, J. Zaanen, and T. P. Devereaux, Systematic study of electron-phonon coupling to oxygen modes across the cuprates, Phys. Rev. B 82, 064513 (2010).
- [55] T. Esslinger, Fermi-Hubbard physics with atoms in an optical lattice, Annu. Rev. Condens. Matter Phys. 1, 129 (2010).
- [56] H. Fehske, G. Wellein, G. Hager, A. Weiße, and A. R. Bishop, Quantum lattice dynamical effects on single-particle excitations in one-dimensional Mott and Peierls insulators, Phys. Rev. B **69**, 165115 (2004).
- [57] W. Hu, B. Gu, and I. Franco, Lessons on electronic decoherence in molecules from exact modeling, J. Chem. Phys. **148**, 134304 (2018).
- [58] J. C. Light and T. Carrington, Discrete-variable representations and their utilization, in *Advances in Chemical Physics* (John Wiley & Sons, Inc., New York, 2007), pp. 263–310, 10.1002/9780470141731.ch4.
- [59] P. Jordan and E. Wigner, Über das Paulische Äquivalenzverbot, Z. Phys. 47, 631 (1928).
- [60] D. T. Colbert and W. H. Miller, A novel discrete variable representation for quantum mechanical reactive scattering via the s-matrix Kohn method, J. Chem. Phys. **96**, 1982 (1992). https://doi.org/10.6084/m9.figshare.28208165.
- [61] https://doi.org/10.6084/m9.figshare.28208165